

Atmospheric Neutrinos

Thomas K. Gaisser

Bartol Research Institute and Department of Physics and Astronomy
University of Delaware, Newark, DE, 19716, USA

E-mail: gaisser@bartol.udel.edu

Abstract. In view of the observation by IceCube of high-energy astrophysical neutrinos, it is important to quantify the uncertainty in the background of atmospheric neutrinos. There are two sources of uncertainty, the imperfect knowledge of the spectrum and composition of the primary cosmic rays that produce the neutrinos and the limited understanding of hadron production, including charm, at high energy. This paper is an overview of both aspects.

1. Introduction

To calculate the spectrum of atmospheric neutrinos up to the PeV range it is necessary to use as input the primary cosmic-ray spectrum to ~ 100 PeV, well into the energy region where data is available only from ground-based air shower experiments. These experiments measure the spectrum of energy per particle. The relative fraction of various nuclei is obtained indirectly from ground-level observables, such as the ratio of electrons to electromagnetic particles, or by comparing the depth of shower maximum to expectation. In both cases the results depend on simulations with event generators that embody the hadronic physics. The composition is important because it is the energy per nucleon that is relevant for the atmospheric neutrino spectrum, rather than the all-particle spectrum measured by the air shower experiments.

Models of the spectrum and composition are anchored to direct measurements which extend to about 100 TeV for protons and helium, but an order of magnitude lower for the carbon group [1]. Fits to direct measurements need to be extrapolated to higher energy and joined to results from air shower experiments, such as KASCADE [2]. The classic example of such a parameterization is the Polygonato Model of Hörandel [3]. Understanding the composition and spectrum through the knee region where the spectrum steepens significantly is crucial for calculating the atmospheric neutrino spectrum above 100 TeV.

These points are illustrated in the first two figures of a paper [4] from TAUP 2013, reproduced here in Fig. 1. Around 30 TeV, the helium contribution, which has a slightly harder spectrum, crosses the proton contribution to the all-particle spectrum. At the same energy per nucleon, however, the contribution of the four nucleons in He to the spectrum of nucleons is about a factor of three below protons.

The plan of this paper is to compare the atmospheric neutrino spectrum using a reference hadronic interaction model with several different models of the primary spectrum in the next section. The following section takes a single model of the primary spectrum and shows the atmospheric neutrino spectrum for several hadronic event generators. Prompt neutrinos and charm are discussed separately in the last section.

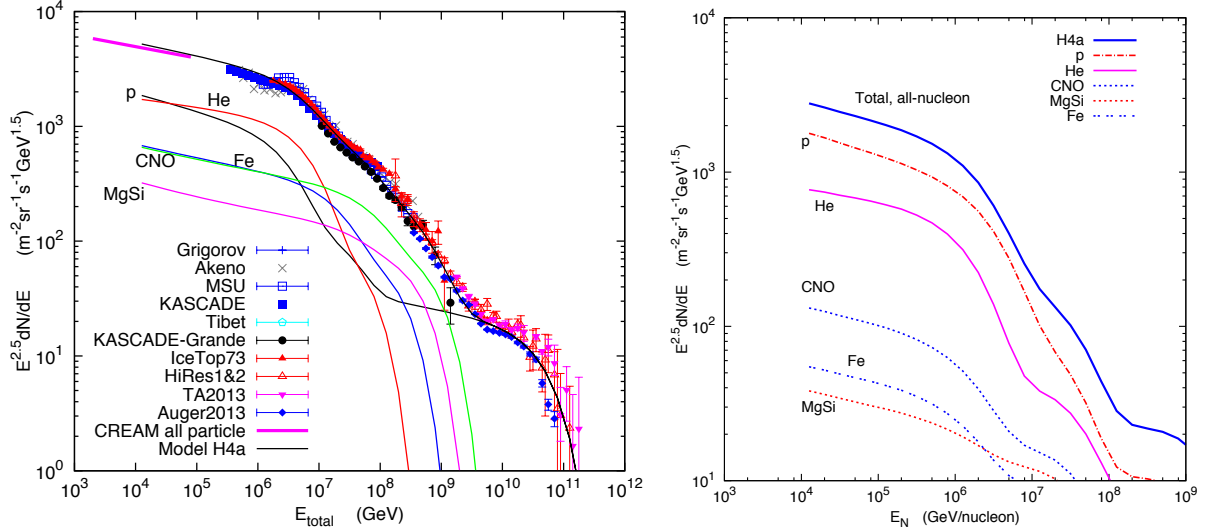


Figure 1. Cosmic ray energy spectrum of nuclei (left) and the corresponding spectrum of nucleons (right)

2. Models of the primary spectrum

The uncertainty in the flux of conventional neutrinos from decay of K^\pm and π^\pm is illustrated in Fig. 2 by comparing the results of five different models of the primary spectrum and composition. All are calculated numerically as described in Ref. [6] using the same hadronic interaction model.

The spectrum models described and tabulated in Ref. [7] are designed to connect with direct measurements below 100 TeV, to describe the knee region, and also to be applicable at the highest energies. The common feature of these models is that they consist of several populations of particles, with successively higher cutoffs in rigidity. In the H3a model [8], for example, each population consists of the five major nuclear groups, represented by p, He, N, Si and Fe. The first population has an exponential cutoff at $R_c = 4$ PV with the spectral index of each mass group tuned to match direct measurements (e.g. [1]). In particular, helium has a harder spectrum in the first population than protons. The second population with $R_c = 30$ PV is a Galactic component of unknown origin that fills the gap that would otherwise occur below the assumed extra-galactic population [9]. In H3a the extra-galactic population contains all nuclei with a cutoff of $R_c = 2$ EV. In the two models introduced in Ref. [7] (GST1 and GST2), the populations above the knee contain no intermediate mass nuclei. As a consequence, the spectrum of nucleons is dominated by protons above $\sim 10^7$ GeV. This feature in the composition of the GST models is reflected in the corresponding neutrino spectra above a few PeV (Fig. 2).

The primary spectrum used for two benchmark calculations of the atmospheric neutrino flux Bartol [10] and Honda [11] is the high-helium version of a spectrum fit given in Ref. [12]. That parameterization was made for energy per nucleon less than ~ 100 TeV. Here, populations 2 and 3 of H3a are used to extend this model (Honda06) through the knee region and beyond. The detailed Polygonato model [3, 13] provides an extrapolation specifically designed to describe the knee in the cosmic-ray spectrum in the PeV energy range, but not for the much higher EeV energy range. Population 3 of H3a is used here to extend the version of Polygonato with a rigidity-dependent cutoff in the knee region to higher energy (“Poly-mod” in Fig. 2). In both cases, the H3a components are renormalized to make a smooth transition.

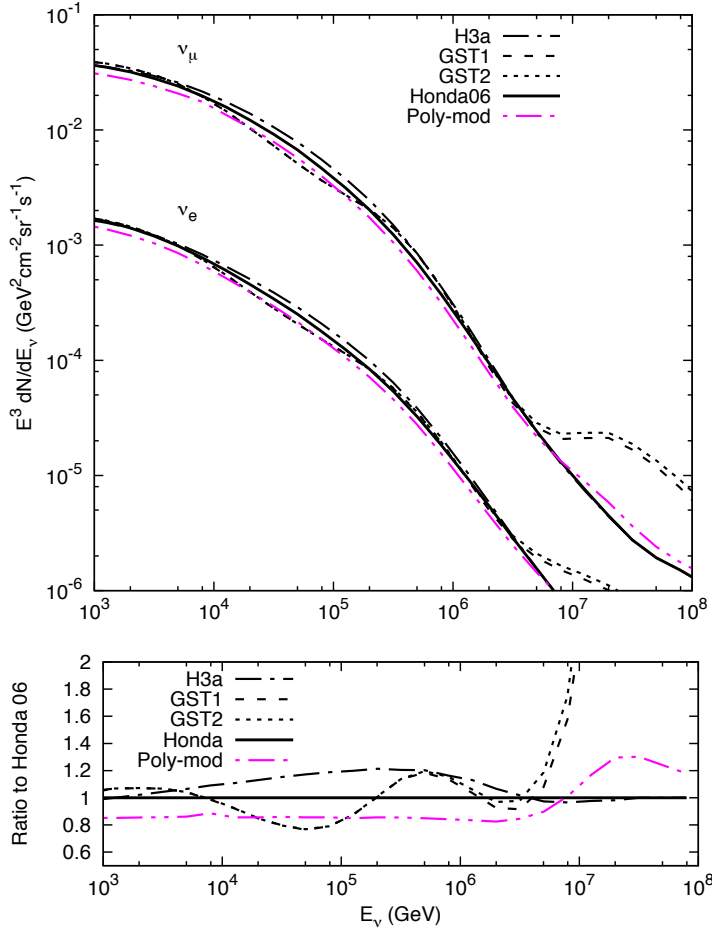


Figure 2. Top panel: Conventional $\nu + \bar{\nu}$ fluxes averaged over all zenith angles for 5 primary spectra calculated with the EPOS-LHC model [5]; Bottom panel: ratio to Honda 06.

3. Hadronic interaction models

Spectrum-weighted moments have been tabulated as a function of beam energy for several interaction models using the CRMC program [14]. The energy-dependent inclusive cross sections are then derived for each model and the neutrino fluxes are calculated using the numerical method of Ref. [15] as described in Ref. [6]. The hadronic interaction models are listed in Table 1. The neutrino fluxes from these models are compared to each other in Fig. 3.

Model	Comment
Scaling	Energy-independent Z -factors from [16]
Honda [17]	Tuned to atmospheric μ^\pm ; used in [11] for atmospheric ν
QGSjet II-04 [18]	Post-LHC version of QGSjet
EPOS LHC [5]	Post-LHC version of EPOS
Sib 2.3 dev [19]	Development version of post-LHC SIBYLL
Sib 2.1 [20]	Pre-LHC Sibyll

Table 1. List of hadronic interaction models for the atmospheric neutrino spectra in Fig. 3.

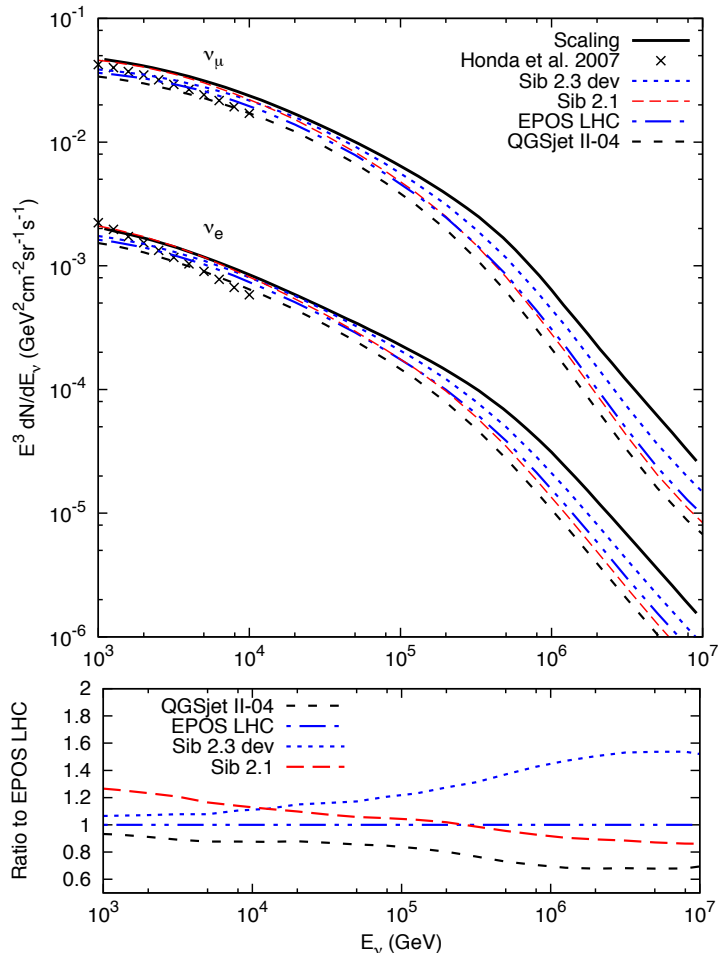


Figure 3. Top panel: Conventional neutrino plus anti-neutrino fluxes averaged over all zenith angles for several interaction models; Bottom panel: Ratios to fluxes calculated with EPOS-LHC. (Note: The numerical calculations shown here by the lines do not include neutrinos from decay of muons, which are negligible for ν_μ with $E > \text{TeV}$. There is still some contribution to TeV ν_e , which probably accounts for the steeper ν_e flux from the tables of Ref. [11], which do include this contribution.)

4. Prompt neutrinos from decay of charm

There are many calculations of the flux of prompt neutrinos from decay of charmed hadrons produced by interactions of cosmic rays in the atmosphere. Several of these are shown in Fig. 4 with solid lines. There are uncertainties in the level of prompt neutrinos related to limited knowledge of production of charmed hadrons and also from the primary spectrum and composition. Examples of both are shown in the figure. The heavy solid lines are from ERS [21] (rescaled to include the effect of the knee) and BERSS [22], both assuming the H3a model for the primary spectrum and composition.

To illustrate the effect of differences in primary spectrum, a simple model of the energy-dependent charm production was made based on Fig. 2 of BERSS [22]. The prompt flux was then calculated using the same numerical method as for the conventional neutrinos, taking account of the much higher critical energies for charmed hadrons (3.84×10^7 GeV for D^\pm and 9.71×10^7 GeV for D^0). The results are shown for spectrum models H3a, H4a and GST1 by the

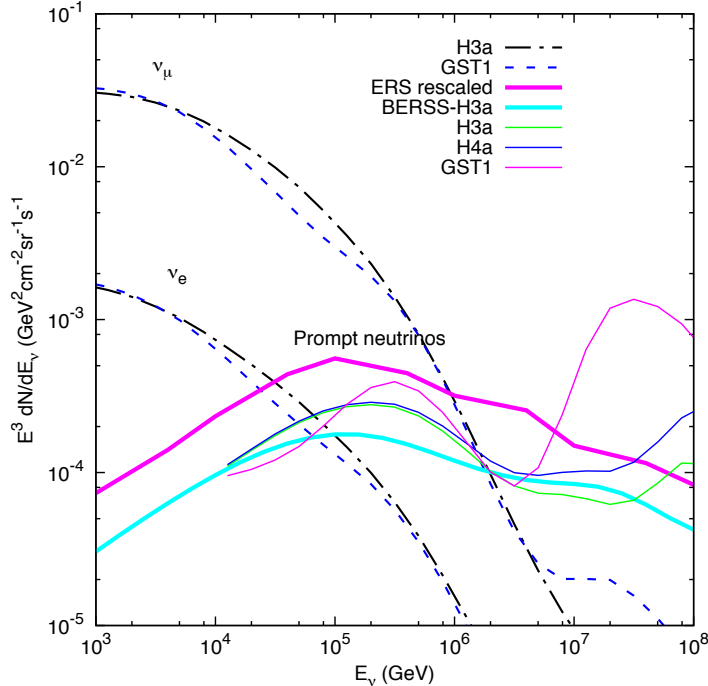


Figure 4. Various estimates of the intensity of prompt atmospheric neutrinos from decay of charm compared to conventional atmospheric neutrinos.

three thin continuous lines in the figure. (H4a differs from H3a only in the 3rd (extragalactic) population, which is all protons for H4a.) For comparison, the fluxes of conventional atmospheric neutrinos are shown by the broken lines for H3a and GST1.

Fluxes of ν_e and ν_μ from decay of charm are nearly equal, unlike the case for conventional neutrinos, for which $\nu_e/\nu_\mu \approx 0.04$. For the examples shown here, the crossover energy at which the prompt neutrino flux becomes larger than the conventional is between 10 and 100 TeV for ν_e and between 1 and 3 PeV for muon neutrinos. The effect of the protons in the GST models is again apparent in the increased intensity above 10 PeV. Sibyll 2.3 [19] includes production of charm and gives a prompt flux within the range shown in Fig. 4.

A new calculation of prompt neutrinos by Garzelli et al. [23] that starts from next to leading order QCD for hadro-production of charm gives results that are similar in magnitude to Fig. 4. Reference [23] (also presented at TAUP 2015) includes an extensive evaluation of uncertainties in the flux of neutrinos from decay of charm. Taken together, the recent calculations are in broad agreement and predict levels of prompt neutrinos within a factor of two of the results shown here.

5. Acknowledgments

I thank Felipe Campos Penha for helpful discussions of lepton fluxes. I thank Hans Dembinski for providing the Z-factors for the various hadronic interaction event generators used in this paper, and I thank Ralph Engel, Anatoli Fedynitch, Felix Riehn and Todor Stanev for helpful discussion on SIBYLL and related topics. This research is supported in part by grants from the U.S. National Science Foundation, NSF-PHY-1205809 and from the U.S. Department of Energy, 12ER41808.

6. References

- [1] Seo E S 2012 *Astropart. Phys.* **39-40** 76–87
- [2] Antoni T *et al.* (KASCADE) 2005 *Astropart. Phys.* **24** 1–25 (*Preprint astro-ph/0505413*)
- [3] Hörandel J R 2003 *Astropart. Phys.* **19** 193–220 (*Preprint astro-ph/0210453*)
- [4] Gaisser T K 2015 *Phys. Procedia* **61** 608–611
- [5] Pierog T, Karpenko I, Katzy J M, Yatsenko E and Werner K 2015 *Phys. Rev.* **C92** 034906 (*Preprint 1306.0121*)
- [6] Gaisser T K 2015 *EPJ Web Conf.* **99** 05002 (*Preprint 1412.6424*)
- [7] Gaisser T K, Stanev T and Tilav S 2013 *Front. Phys. China* **8** 748–758 (*Preprint 1303.3565*)
- [8] Gaisser T K 2012 *Astropart. Phys.* **35** 801–806
- [9] Hillas A M 2005 *J. Phys.* **G31** R95–R131
- [10] Barr G D, Gaisser T K, Lipari P, Robbins S and Stanev T 2004 *Phys. Rev.* **D70** 023006 (*Preprint astro-ph/0403630*)
- [11] Honda M, Kajita T, Kasahara K, Midorikawa S and Sanuki T 2007 *Phys. Rev.* **D75** 043006 (*Preprint astro-ph/0611418*)
- [12] Gaisser T K, Stanev T, Honda M and Lipari P 2001 *27th International Cosmic Ray Conference (ICRC 2001) Hamburg, Germany, August 7-15, 2001* pp 1643–1646
- [13] Hörandel J R 2004 *Astropart. Phys.* **21** 241–265 (*Preprint astro-ph/0402356*)
- [14] Pierog T, Baus C and Ulrich R URL <https://web.ikp.kit.edu/rulrich/crmc.html>
- [15] Thunman M, Ingelman G and Gondolo P 1996 *Astropart. Phys.* **5** 309–332 (*Preprint hep-ph/9505417*)
- [16] Gaisser T K 1990 *Cosmic rays and particle physics*, Cambridge University Press
- [17] Sanuki T, Honda M, Kajita T, Kasahara K and Midorikawa S 2007 *Phys. Rev.* **D75** 043005 (*Preprint astro-ph/0611201*)
- [18] Ostapchenko S 2013 *EPJ Web Conf.* **52** 02001
- [19] Riehn F, Engel R, Fedynitch A, Gaisser T K and Stanev T 2015 (*Preprint 1510.00568*)
- [20] Ahn E J, Engel R, Gaisser T K, Lipari P and Stanev T 2009 *Phys. Rev. D* **80** 094003 (*Preprint 0906.4113*)
- [21] Enberg R, Reno M H and Sarcevic I 2008 *Phys. Rev.* **D78** 043005 (*Preprint 0806.0418*)
- [22] Bhattacharya A, Enberg R, Reno M H, Sarcevic I and Stasto A 2015 *JHEP* **06** 110 (*Preprint 1502.01076*)
- [23] Garzelli M V, Moch S and Sigl G 2015 *JHEP* **10** 115 (*Preprint 1507.01570*)